Machine Recognition of Weevil Damage in Wheat Radiographs

P. M. KEAGY and T. F. SCHATZKI[1]

ABSTRACT

An image processing algorithm was developed for machine recognition of weevils and/or weevil damage in digitally scanned film radiographs (8 bits, $[0.25\ mm]^2$/pixel) of wheat kernels containing granary or maize weevils. The gray scale image is converted to a binary image of interior edges, lines, and cavities using a Laplacian mask, zero threshold, and background removal. In undamaged kernels, the predominant feature of this image is a line representing the central crease of the kernel. In insect-damaged kernels, this feature is disrupted, and additional edges or lines are seen at angles to the crease. The algorithm uses convolution masks to look for such intersections (45 or 90° angles with 4- or 5-pixel length sides) at eight orientations. Recognition varies with insect stage; at least 50% of infested kernels are machine recognized by the 4th instar (26–28 days). This is comparable to 50% recognition by humans at 25.5 days for images of similar resolution. False positive responses are limited to 0.5%.

Cereal Chem. 70(6):696–700

The rapid development of computerized image acquisition and processing has led to the automation of many repetitive inspection tasks that formerly depended on human inspectors. Image acquisition and processing techniques are being developed for applications in the grain industry such as type classification of wheat kernels (Zayas et al 1985, 1986; Neuman et al 1987; Sapirstein et al 1987; Symons and Fulcher 1988a,b; Chen et al 1989; Thomson and Pomeranz 1991), determination of grades within a type (Sapirstein et al 1991), recognition of seed shape (Travis and Draper 1985), and evaluation of bread crumb grain features (Sapirstein et al 1992; Zayas 1992).

Detection and control of hidden insects during grain storage and commerce is a major problem for the cereal and milling industry (Storey et al 1982). Present USDA standards apply only to live external insects (USDA/FGIS 1987, 1992), which are observed visually after sifting. Such methods do not detect insects hidden within kernels, which are the main source of insect fragments in flour (Harris et al 1952). Weevils, notably in the family Curculionidae, develop from egg to adult entirely inside grain kernels and are extremely important pests of stored grain. A number of methods for detecting such insects have been proposed or are in development (Arteman 1982, Schatzki and Fine 1988, Keagy and Schatzki 1991). Among those, radiography has found the greatest acceptance (Arteman 1982), presumably because it is simple, relatively fast, and definitive for older hidden insects (Russell 1988, Keagy and Schatzki 1991).

Because of the expense of film radiography and the subjectivity of human visual inspection (Keagy and Schatzki 1991), it would be desirable to develop an automated inspection system for hidden insects. Machine recognition software would be required. Stermer (1973) reported a prototype of a system using potassium-carbonate-treated kernels to enhance X-ray contrast of infested kernels. The lengthy potassium carbonate treatment probably discouraged adoption of that system.

In the present work, machine-generated images were not available. Therefore, low-resolution images derived from film were used to simulate X-ray imaging hardware. The natural contrast produced by soft X-rays is enhanced by image processing. Abnormal interior "edges" (referring, in this article, either to edges in the usual terminology, as boundaries between two regions of differing intensity, or to lines) are detected by a recognition algorithm for hidden weevils in wheat. Such algorithms can then serve as prototypes for an automated system. The mechanical and electrical engineering aspects of such a system are not addressed in this article.

[1] U.S. Department of Agriculture, Agricultural Research Service, Western Regional Research Center, Albany, CA 94710.

Mention of firm names or trade products does not imply that they are endorsed or recommended by the U.S. Department of Agriculture over other firms or products not mentioned.

MATERIALS AND METHODS

Infested Kernel Images

Sitophilus granarius L. (granary weevils) were obtained from W. Burkholder, University of Wisconsin, and maintained on wheat at 75% rh, 25°C. Clean hard red wheat (50 g), obtained from a commercial mill, was exposed to 50 unsexed adults (one adult per gram of wheat) for three days, after which the adults were removed. Eighteen days after initial insect exposure, the wheat kernels were X-rayed (2 min at 20 keV [0.25 mm Be window], with a Faxitron series X-ray system 4380N, Hewlett Packard, McMinnville, OR; Industrex B film, Eastman Kodak, Rochester, NY). The films were visually inspected, and 93 kernels that appeared to contain weevil larvae were selected. The selected kernels were arranged in a nonoccluding manner on clear contact paper (Rubbermaid Inc., Wooster, OH) attached to a metal picture frame. The kernels were oriented lengthwise and randomly positioned either crease up or crease down. The tray containing these kernels was placed within two plastic ziplock bags to retain emerging adults and returned to the incubator for further weevil development. Radiographs of the tray were made at intervals of one to three days until the weevils emerged. Mature weevils emerged from 87 of the 93 kernels. Four kernels were not infested; one weevil developed late; and one weevil ceased development. A plastic step wedge (layers of plexiglass combined to give thicknesses of 0.113, 0.172, 0.223, 0.279, and 0.335 mm) was included in each X-ray image as an X-ray absorption standard.

Images of 56 wheat kernels infested with maize weevils (*S. zeamais* Motsch.), were available from the images previously imaged at $(0.033\ mm)^2$/pixel and were studied by Keagy and Schatzki (1991). These images were processed here at a resolution of $(0.262\ mm)^2$/pixel.

To evaluate the rate at which noninfested kernels were falsely recognized as infested kernels, 6,727 kernels of clean commercial hard red wheat were X-rayed as described above. An additional 1,040 noninfested kernel images were available from the set described by Keagy and Schatzki (1991).

Life Stages

Life stage (stadium) of each insect was determined by comparing features seen on the X-ray radiograph to standard criteria. The classification followed essentially that of Kirkpatrick and Wilbur (1965) except that cavity width, rather than tunnel width or head capsule size, were used to classify instars; the latter sizes were not always easily measured in X-ray views. Mean duration of each stadium at 26.6°C. and 70% rh in days is: first instar, 4.5; second instar, 4.7; third instar, 6.2; fourth instar, 6.9; prepupa, 0.7; pupa, 6.5; and preadult, 6.3 (Kirkpatrick and Wilbur 1965; Schatzki et al 1993). As a result of differences in duration, all life stages are not equally represented in the image data set.

Image Acquisition System

The image acquisition system, for obtaining images of granary-weevil-infested kernels from X-ray film, consisted of a digital

CCD video camera (Videk, Canandaigua, NY; Megaplus model K5004; 1,024 × 1,280 pixels; 256 levels of gray) with a Nikon *f*2.8, 55-mm lens and 0.9 neutral-density filter, mounted 0.71 m above a fan-cooled light box on which the X-ray film was placed. In the resulting image, one square pixel corresponded to (0.085 mm)^2 of film. The light box illuminating the film consisted of a frosted glass surface over eight F15T8 GE cool white fluorescent light bulbs driven at 60 kHz by two Mercron lamp-controllers (model HR06120-4, Richardson, TX). The Mercron AC power supplies provide ripple-free light regulated within 1%. Light output is set by potentiometers (variable between 30 and 550 mA) inside the controllers. Ambient light was excluded by a black corduroy curtain sealed against light at the light box and camera lens.

Exposure at *f*4 for 0.06 sec was found adequate to yield a maximum gray level intensity of 255 (showing the thickest part of the largest kernels). This exposure was kept constant for all images and checked routinely for uniformity with the plastic wedge. Under these conditions, fully exposed film (background) yielded a gray level intensity of approximately 13 (see below). The digital image produced by the camera was transferred to an asynchronous input module (Max Scan, DataCube, Peabody, MA) mounted on the VME bus of a Sun 4/470 workstation (Sun Microsystems, Inc., Mountain View, CA). The HIPS image processing package (SmartImage Software, New York) running on the Sun workstation was used to develop the weevil recognition algorithm. To simulate lower-resolution images acquired by a 0.25- × 0.25-mm phosphor-coated photodiode sensor such as might be installed in an X-ray linescan device, the Videk images were reduced by a factor of three by pixel averaging (one pixel width = 3 × 0.085 mm).

Algorithm Description

Figure 1 (rows 1 and 4) shows the high-resolution ([0.033 mm]^2/pixel) film images of a typical wheat kernel infested with maize weevils at increasing insect age. The same images reduced to (0.25 mm)^2 resolution and then enlarged are shown in rows 2 and 5.

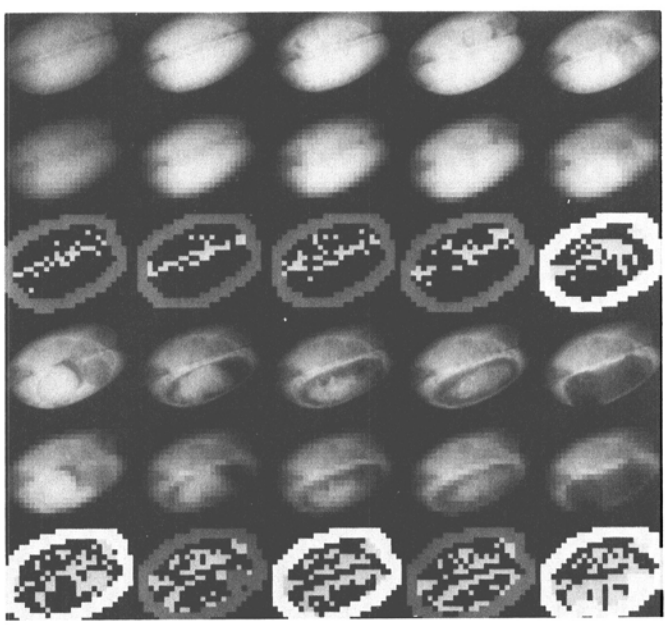

Fig. 1. Typical maize weevil images. Rows 1 and 4 are wheat kernels shown at (0.033 mm)^2/pixel resolution and containing, in row 1 (left to right): weevils at first instar (day 10), second instar (day 14), third instar (day 17), third instar (day 21), third/fourth instar (day 24); in row 4: weevils at fourth instar (day 28), pupa stage (day 31), pupa stage (day 35) and preadult stage (day 38), and an empty kernel (day 42). Rows 2 and 5 are the same images reduced to simulate (0.25 mm)^2/pixel resolution, then enlarged for illustration. Rows 3 and 6 are binary images produced from rows 2 and 5. Off-white interior pixels mark interior edges. White kernel outlines indicate kernels recognized as infested. Dark gray outlines indicate kernels not recognized as infested.

The latter are the images available for computer recognition and are referred to here as the gray-level images.

In sound kernels or those infested with very young insects, the predominant features of the kernel are the central crease, germ region, and border of the kernel. In kernels infested with older insects, the developing insect and interior cavities created by the insect become more prominent and sometimes obliterate the original crease and germ features. These features, made obvious by adjacent regions of light and dark pixels, need to be segregated to extract the insect-created features. A model of an infested kernel consists of an X-ray-absorbing insect placed in a nonabsorbing cavity, which is contained in an absorbing kernel, which, finally, is surrounded by a nonabsorbing background. The second derivative, or more generally the Laplacian, $\partial^2/\partial x^2 + \partial^2/\partial y^2$, of the gray level intensity profile of the kernel cross-section is positive only in the region corresponding to the cavity between the insect and the kernel and at the exterior edges of the kernel itself. In the case of more mature insects, having outlines more complex than those of larvae, the cavities have more complex shapes as well, but the same arguments apply. These cavities are prime indicators of infestation. Use of the derivative assures that this result is independent of the actual intensity values, an advantage that has been exploited in other image-processing problems (e.g., Schatzki et al 1983). If the Laplacian is computed and only the positive values are kept, the output image contains only the outline of the kernel with the interior cavities. This binary image (1, where the Laplacian is positive and 0 elsewhere) is referred to here as the Laplacian edge image. An additional feature also exhibits a positive Laplacian, i.e., the crease in the kernel. The two confounding regions, outer edge and crease, need to be excluded when the Laplacian edge image is used in detecting infestation.

In a sound kernel, the Laplacian edge image shows the crease as an isolated, narrow line. Masks that cover wide regions but exclude narrow ones can be used to detect cavities selectively. The outer edge of the kernel can be distinguished (and thus removed) by recognizing its proximity to the background between the kernels. This forms the basis for the algorithm: generate the Laplacian (binary) edge, establish the background level, remove the kernel outer edge (by its proximity to the background region), and look for extended (wide) regions by the use of appropriate masks. If the latter are found, the kernel is classified as infested. The germ boundary occasionally also shows a positive Laplacian and thus can cause false positives when intersected by the crease. However, this is rare enough not to cause a major problem.

To remove the pixels due to the kernel edge, the gray level value (threshold level) of the substantially constant dark region corresponding to the space between kernels was empirically determined using an interactive image display program. A binary image was then created with pixels set to 0 for source-image pixels darker than the threshold level (the gray level was 13), while the value was set to 1 for brighter pixels. This was termed the black and white image. The boundary between these regions was easily established with a 3 × 3 Sobel edge detector (Gonzalez and Wintz 1987). Any pixel that corresponded to a boundary pixel in the black and white image was eliminated from the Laplacian edge image. The result was defined as the interior edge image.

For most kernels, the interior edge image contained a central line of pixels corresponding to the crease and, for infested kernels, additional pixels associated with the outline of an insect and/or any cavities. The masks used to detect these cavities were chosen to represent the crease plus additional pixels not normally present in uninfested kernel images. Figure 2 shows the 16 masks used. Taken together, the masks show rotational symmetry, they represent all orientations of 45 and 90° angles that can be accommodated within 5 × 5 or 7 × 7 masks. Masks containing angles with sides of less than four or five pixels generated excessive numbers of false positives. Other masks may be equally or more effective at detecting insects; however, the need for minimal false positive responses eliminated many otherwise attractive masks. The 16 masks were passed over the interior edge image, one at

a time, to search for any match where all pixels of the mask corresponded to pixels in the edge image. When a match was found, the kernel was identified as infested. In Figure 1, the interior edge image is shown in rows 3 and 6 as off-white interior pixels, while the outline region, which had been subtracted from the original Laplacian edge image is shown as an exterior band. If the kernel was identified as infested, the outline is shown in white (fifth kernel of row 3; first, third, and fifth kernels of row 6); if it was not so identified, a gray outline is shown. The algorithm is outlined as a block diagram in Figure 3.

Image Translation

The question arises of what happens when an image edge falls entirely within one pixel or is contained partially in each of two adjacent pixels. The image reduction provided the opportunity to explore this question. When the images were reduced by a factor of three to simulate the resolution of a 0.25-mm linescan sensor, a square array of nine pixels was averaged to output one new pixel. There are thus nine separate possible alignments of pixels at the start of each reduction operation. This averaging was used to study the effect of random positioning of kernels with respect to large linescan X-ray sensors. The radiograph representing 25- to 28-day-old granary weevils (93 kernels containing 88 weevils) was reduced using each of the nine possible pixel groupings. The frequency of recognition of each kernel was then determined.

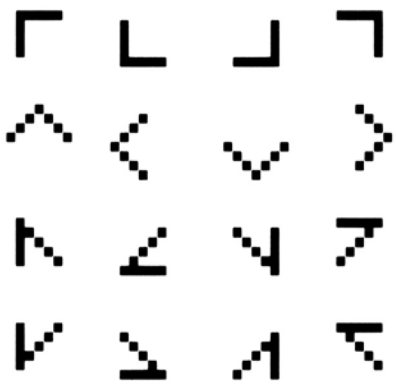

Fig. 2. Convolution masks used to recognize weevil-damaged wheat kernels.

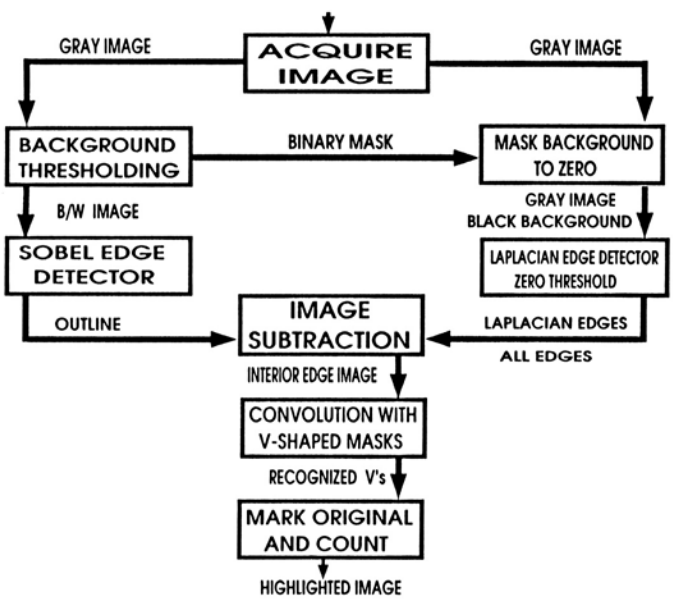

Fig. 3. Block diagram of image processing steps used in machine recognition of weevil-damaged wheat. B/W = black and white.

Image Rotation

The same radiograph of 25- to 28-day-old granary weevils was used to test the effect of image rotation on the algorithm. This image was rotated through 0, 11, 22, 34, or 45° using the HIPS rotate command; the recognition algorithm was applied to the resulting images; and the frequency of recognition of each kernel was then determined.

Statistical Analysis

The least squares model in the CATMOD procedure of the Statistical Analysis System (SAS 1988) was used to obtain the proportion (marginal probability) and standard error of infested kernels identified as a function of insect stage.

RESULTS AND DISCUSSION

Weevil Recognition

Table I gives the proportion of infested kernels identified by the computer algorithm as a function of developmental stage for two species of weevils grown in two separate lots of wheat. Machine recognition increased with each succeeding larval stage from the second instar through the fourth instar. Recognition decreased at the prepupa (maize weevil) or pupa (granary weevil) stages and then increased again at the preadult stage. The pattern is similar for both weevils, with the maize weevil showing lower recognition overall.

Increasing recognition with increasing age was demonstrated for human visual detection of weevils by Schatzki and Fine (1988). This is largely a function of target size (Schatzki and Keagy 1991). Differences in recognition of maize and granary weevil images may thus be due to the larger size of granary weevils. Maize weevil tunnels average 69–75% of the width of granary weevil tunnels for the first through fourth instars (Kirkpatrick and Wilbur 1965, Sharifi and Mills 1971). Machine recognition levels at the fourth instar stage (72% recognition of granary weevils at 26 days of age, 50% recognition of maize weevils at 28 days of age) are similar to the 50% human recognition of maize weevils at 25 days of age found earlier at similar image resolution ([0.262 mm]^2/pixel; Keagy and Schatzki 1991). Unlike human visual detection, machine recognition decreases at the prepupal stage for maize

TABLE I
Machine Recognition of Wheat Kernels Infested with Maize and Granary Weevils, by Stage

Stage[a]	Proportion Recognized[b]	Insect Age[c]	n[d]
Maize weevil			
No insect	0.006 ± 0.002		1,040
1st instar	0.05 ± 0.03	11.7 ± 0.5	41
2nd instar	0.05 ± 0.02	15.9 ± 0.3	78
3rd instar	0.17 ± 0.04	21.3 ± 0.3	103
4th instar	0.51 ± 0.05	28.1 ± 0.3	99
Prepupa	0.22 ± 0.10	32.1 ± 0.7	18
Pupa	0.36 ± 0.05	34.2 ± 0.3	84
Preadult	0.53 ± 0.05	39.8 ± 0.3	97
Empty kernel	0.77 ± 0.05	43.9 ± 0.4	62
Granary weevil			
No insect	0.005 ± 0.001		6,727
2nd instar	0.06 ± 0.02	17.0 ± 0.3	157
3rd instar	0.12 ± 0.02	20.9 ± 0.2	345
4th instar	0.72 ± 0.03	26.2 ± 0.2	278
Prepupa	0.85 ± 0.04	30.3 ± 0.4	79
Pupa	0.47 ± 0.03	34.2 ± 0.2	284
Preadult	0.77 ± 0.03	39.7 ± 0.2	226
Empty kernel	0.86 ± 0.04	43.1 ± 0.2	90

[a] Developmental stage was determined as described by Kirkpatrick and Wilbur (1965). Mean stadium (period between any two successive molts) in days is 4.5, 4.7, 6.2, 6.9, 0.7, 6.5, and 6.3 for first instar, second instar, third instar, fourth instar, prepupa, pupa, and preadult stages, respectively (Kirkpatrick and Wilber 1965; Schatzki et al 1993).
[b] Fraction of total kernels of each stadium recognized ± standard error.
[c] Average age in days of insects of each stadium ± standard error.
[d] Total number of kernel images containing insects within each stadium.

weevils. At this stage, the kernel crease line had usually been obliterated by the insect and was no longer present to form one of the intersecting lines matched by the convolution masks. Consequently, a mask specifically designed to detect this stage is needed.

False Positive Rate

Of 1,040 noninfested images obtained with the maize weevil image set, six kernels (0.6%, 95% upper confidence limit = 1.1%) were falsely identified as infested. These images were examined to determine the source of the misclassification. In five cases, an identifiable image feature generated an internal kernel edge, causing the false classification. Two kernels contained cracks; two had long, relatively straight germ borders; one contained an area of decreased endosperm density; and for one kernel no apparent cause was observed.

To obtain a better sample of the causes of false positive classifications, a larger number of noninfested kernel images was obtained with the granary weevil set. Of 6,727 kernels of clean commercial wheat, the recognition algorithm falsely determined 32 kernels (0.5%, 95% upper confidence limit = 0.64%) to be infested. Individual examination of the 32 original and binary images revealed 10 kernels with interior cracks, two with interior damage, 14 with areas of decreased density within the endosperm, one that was shriveled, and five in which the border of the germ and endosperm was mistaken for infestation. Similar seed characteristics that resembled insect damage were noted by Nicholson et al (1953).

There are currently no quality standards for hidden insects in grain. The U.S. Food and Drug Administration considers flour unacceptable for human consumption when the number of insect fragments exceeds 75 per 50 g (U.S. FDA 1988). Using the cracking and flotation method, Harris et al (1952) found that wheat containing an average of 8.5 whole or equivalent insects per 100 g of uncleaned wheat produced flour containing 61–80 insect fragments per 50 g of flour. However, the relationship between insects in grain and fragments in flour is difficult to establish; it is known to depend on the age of the immature insect and whether it is alive or dead (Sachdeva 1978). Eggs and larvae add few insect parts to flour since only insects in the pupa through adult stages are highly sclerotized. From experience, millers will tend to accept wheat when X-ray shows fewer than five or six hidden insects per 50 g (approximately 1,500 kernels). This size sample of clean wheat will contain approximately seven to nine false positive responses due to cracks and other grain defects. Therefore, it is necessary to use a secondary method such as ninhydrin staining (Dennis and Decker 1962) of suspect kernels to confirm infestation when the level of infestation is borderline.

Effect of Image Translation

As noted above, nine distinct translational shifts (alignments) are possible when an image is reduced threefold horizontally and vertically. The number of kernels producing each of the 10 possible recognition frequencies from 0 (never recognized) to 9 (always recognized) are shown in Table II.

Of the 88 infested kernels in the image, 12 corresponded to the third instar (stage 3), of which eight were never recognized regardless of alignment. Eight corresponded to the prepupa stage (stage 5), of which six were always recognized. Therefore, for the easy (or difficult) to recognize stages, alignment is not a problem. Alignment dependence is most critical for the remaining 68 kernels corresponding to the fourth instar (stage 4), where recognition is only partial. Of these 68, a total of 36 were either never recognized (11) or always recognized (25). Thus for 52% of these images (36/68) the algorithm is alignment independent, whereas for another 26% (18/68) the same thing is largely true (they were recognized seven or more times out of nine, or two or less times out of nine). Thus, the algorithm is translation independent for one half of the images of the difficult to recognize stages and substantially independent for three quarters of them.

This same procedure was used for the 32 false positive kernels identified above in the 6,727 kernel sample set. The results (Table III) show a more even distribution of repeated recognition frequencies among false positive kernels. This distribution was used to predict that 13 of the 32 kernels would be classified as infested if they were imaged and subjected to the recognition algorithm again. (Multiply the number of recognitions per kernel in column 1 by the number of kernels in column 2. Sum the results and divide by 9 [nine possible alignments].) This would reduce the false positive rate to 0.2% for this lot of wheat. At the same time, recognition of less-mature infested kernels would also be reduced, as indicated by the data in Table II.

Effect of Image Rotation

When the image of 88 25- to 28-day-old, granary weevil-infested kernels was rotated through 0, 11, 22, 34, or 45°, the total number of kernels recognized was 55, 51, 52, 53, and 53, respectively, using the 16 masks described above. Attempts to remove any row of the masks shown in Figure 2 from the recognition algorithm led to reduced recognition at one or more image rotation angles. This indicates that the 16 masks were both necessary and sufficient to make the algorithm rotation independent for groups of kernels.

The distribution of recognition frequencies from 0 (never recognized) to 5 (always recognized) for individual kernels is summarized in Table IV. Most (59%) of the kernels were rotation independent in that they were consistently always or never recognized. The remaining kernels were sometimes affected by rotation (as they were by translation), with recognition frequencies between 1 and 4. However, as a group, the proportion recognized remained relatively unaffected by rotation.

It is clear from Tables II–IV that machine recognition of an insect is a chance event. The probability of recognition increases with increasing maturity of the insect and associated damage to the wheat kernel. Recognition of individual kernels may be affected by random positioning, but with adequate sample size the proportion recognized is relatively unaffected.

TABLE II
Effect of Variations in Pixel Alignment on Number of 25- to 28-Day-Old Granary Weevil-Infested Wheat Kernels Recognized

Number of Times[a] Recognized in Nine Alignments	Stage[b]			
	3	4	5	All
0	8	11	1	20
1	0	3	0	3
2	1	6	0	7
3	1	4	0	5
4	1	4	0	5
5	1	4	0	5
6	0	2	1	3
7	0	6	0	6
8	0	3	0	3
9	0	25	6	31
Total	12	68	8	88

[a] 0 (never recognized) to 9 (always recognized).
[b] Stage 3 = third instar, 4 = fourth instar, 5 = prepupa.

TABLE III
Effect of Variations in Pixel Alignment on False Recognition of Uninfested Wheat Kernels

Number of Recognitions per Kernel	Kernels	Percent
0	1	3.1
1	9	28.1
2	5	15.6
3	3	9.4
4	1	3.1
5	5	15.6
6	0	0.0
7	3	9.4
8	5	15.6
9	0	0.0
Total	32	100.0

TABLE IV
Effect of Rotation Through 0, 11, 22, 34, or 45 Degrees on Number of 25- to 28-Day-Old Granary Weevil-Infested Wheat Kernels Recognized

Number of Times[a] Recognized in Five Orientations	Stage[b]			
	3	4	5	All
0	6	12	0	18
1	1	6	1	8
2	1	6	0	7
3	3	5	2	10
4	0	11	0	11
5	1	28	5	34
Total	12	68	8	88

[a] 0 (never recognized) to 5 (always recognized).
[b] Stage 3 = third instar, 4 = fourth instar, 5 = prepupa.

CONCLUSIONS

This work demonstrates the potential for machine recognition of hidden weevils at the prepupa stage or later using sensors capable of a resolution of 0.25 mm^2/pixel. A false positive rate of 0.5% indicates the need for additional verification of kernels predicted to be insect infested. The requirements of an automated image-acquisition system have been discussed previously (Keagy and Schatzki 1991). The present algorithm would form the basis for such a system.

ACKNOWLEDGMENTS

We would like to thank Ron Haff for excellent technical assistance.

LITERATURE CITED

ARTEMAN, R. L. 1982 The detection of internal insect infestation in grain. U.S. Dept. Agric., Fed. Grain Insp. Serv. Rep. 81-22-1. The Service: Washington, DC.

CHEN, C., CHIANG, Y. P., and POMERANZ, Y. 1989. Image analysis and characterization of cereal grains with a laser range finder and camera contour extractor. Cereal Chem. 66:466.

DENNIS, N. M., and DECKER, R. W. 1962. A method and machine for detecting living internal insect infestation in wheat. J. Econ. Entomol. 55:199.

GONZALEZ, R. C., and WINTZ, P. 1987. Digital Image Processing. Addison-Wesley: New York.

HARRIS, K. L., NICHOLSON, J. F., RANDOLPH, L. K., and TRAWICK, J. L. 1952. An investigation of insect and rodent contamination of wheat and wheat flour. J. Assoc. Off. Agric. Chem. 38:115.

KEAGY, P. M., and SCHATZKI, T. F. 1991. Effect of image resolution on insect detection in wheat radiographs. Cereal Chem. 68:339.

KIRKPATRICK, R. L., and WILBUR, D. A. 1965. The development and habits of the granary weevil, *Sitophilus granarius* within the kernel of wheat. J. Econ. Entomol. 58:979.

NEUMAN, M., SAPIRSTEIN, H., SHWEDYK, E., and BUSHUK, W. 1987. Discrimination of wheat class and variety by digital image analysis of whole grain samples. J. Cereal Sci. 6:125.

NICHOLSON, J. F., MILNER, M., MUNDAY, W. H., KURTZ, O. L., and HARRIS, K. L. 1953. An evaluation of five procedures for the determination of internal insect infestation of wheat. V. The use of x-rays. J. Assoc. Offic. Agric. Chem. 36:150.

RUSSELL, G. E. 1988. Evaluation of four analytical methods to detect weevils in wheat: Granary weevil *Sitophilus granarius* (L.) in soft wheat. J. Food Prot. 51:547.

SACHDEVA, A. S. 1978. Effect of infestation, stage, form and treatment on fragment count in flour. M.S. thesis, Kansas State University, Manhattan.

SAPIRSTEIN, H., NEUMAN, M., WRIGHT, E. H., SHWEDYK, E., and BUSHUK, W. 1987. An instrumental system for cereal grain classification using digital image analysis. J. Cereal Sci. 6:3.

SAPIRSTEIN, H. D., KOHLER, J. M., and BUSHUK, W. 1991. Discrimination of commercial grades of hard red spring wheat by digital image analysis. (Abstr.) Cereal Foods World 36:685.

SAPIRSTEIN, H. D., INOUE, Y., and BUSHUK, W. 1992. Instrumental measurement of bread crumb grain features by digital image analysis. (Abstr.) Cereal Foods World 37:552.

SAS Institute. 1988. SAS/STAT User's Guide. Release 6.03 edition. The Institute: Cary, NC.

SCHATZKI, T. F., and FINE, T. A. B. 1988. Analysis of radiograms of wheat kernels for quality control. Cereal Chem. 65:233.

SCHATZKI, T. F., and KEAGY, P. M. 1991. Effect of image size and contrast on the recognition of insects in radiograms. SPIE — The International Society for Optical Engineering Proceedings 1379: Optics in Agriculture. J. A. DeShazer and G. E. Mayer, eds. The International Society for Optical Engineering, Bellingham, WA.

SCHATZKI, T. F., GROSSMAN, A., and YOUNG, R. 1983. Recognition of agricultural objects by shape. IEEE Trans. Pattern Recogn. Mach. Intel. 5:645-653

SCHATZKI, T. F., WILSON, E. K., KITTO, B., BEHRENS, P., and HELLER, I. 1993. Determination of hidden *S. granarius* (Coleoptera: Curculionidae) in wheat by myosin ELISA. J. Econ. Entomol. 85:1584.

SHARIFI, S., and MILLS, R. B. 1971. Radiographic studies of *Sitophilus zeamais* Mots. in wheat kernels. J. Stored Prod. Res. 7:195.

STERMER, R. A. 1973. Automated x-ray inspection of grain for insect infestation. Trans. ASAE 15:1081.

STOREY, C. L., SAUER, D. B., ECKER, O., and FULK, D. W. 1982 Insect infestations in wheat and corn exported from the United States. J. Econ. Entomol. 75:827.

SYMONS, S. J., and FULCHER, R. G. 1988a. Determination of wheat kernel morphological variation by digital image analysis: I. Variation in eastern Canadian milling quality wheats. J. Cereal Sci. 8:211.

SYMONS, S. J., and FULCHER, R. G. 1988b. Determination of wheat kernel morphological variation by digital image analysis: II. Variation in cultivars of soft white winter wheats. J. Cereal Sci. 8:219.

THOMSON, W. H., and POMERANZ, Y. 1991. Classification of wheat kernels using three-dimensional image analysis. Cereal Chem. 68:357.

TRAVIS, A. J., and DRAPER, S. R. 1985. A computer based system for the recognition of seed shape. Seed Sci. Technol. 13:813.

USDA/FGIS. 1987. Federal Register 52(125):24432, 24438.

USDA/FGIS. 1992. Wheat, Section 13.3 in Grain Inspection Handbook. Book 2. U.S. Dept. Agric., Fed. Grain Inspect. Serv., Washington, DC.

U.S. FDA. 1988. Compliance policy guides. Section 7104.06. Office of Enforcement, Division of Compliance Policy, U.S. Food and Drug Admin., Washington, DC.

ZAYAS, I. 1992. Potential of digital imaging for bread crumb grain evaluation. (Abstr.) Cereal Foods World 37:552.

ZAYAS, I., POMERANZ, Y., and LAI, F. S. 1985. Discrimination between Arthur and Arkan wheats by image analysis. Cereal Chem. 62:478.

ZAYAS, I., LAI, F. S., and POMERANZ, Y. 1986. Discrimination between wheat classes and varieties by image analysis. Cereal Chem. 63:52.

[Received November 2, 1992. Accepted August 20, 1993.]